

CHARACTERIZATION of a 5.8 GHz 4-STAGE DICKSON CHARGE PUMP with RESISTIVE LOADS

LAURA BLANCA-PIMENTEL
JOE GONZALEZ
MATIAS ALMADA
JESSICA T. BLOCK

SCHOOL OF ELECTRICAL AND
COMPUTER ENGINEERING

DR. GREGORY DURGIN
ADVISOR



INTRODUCTION

As the world's population continues to expand, resources must be managed more efficiently in order to conserve the limited quantities available. Innovations such as the smart grid and wireless sensor networks (WSN) are currently being researched and deployed in order to more effectively monitor energy consumption and production. These networks are capable of providing large amounts of information from spatially distributed sensors. Furthermore, these WSNs are used for monitoring ecosystems and water quality, and they have applications in healthcare, military, and security (Akyildiz, 2001). Radio-frequency identification (RFID) technology is an attractive option for use in WSNs because of simplicity, low-cost, and maintenance free operation (Finkenzeller, 2003).

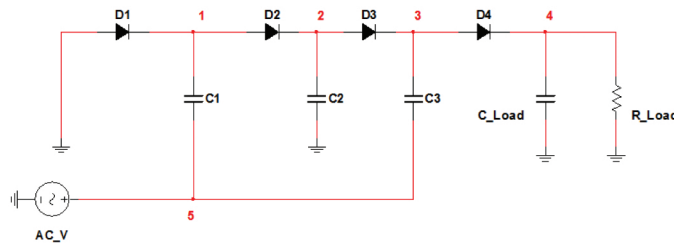
RFID technology is currently used in a wide variety of applications including electronic vehicle registration, toll road payments, public transit payments, product tracking, animal identification, inventory systems, passports, and student IDs (Lee, 2010). These applications require exceedingly small amounts of power to operate because of the need to only transmit identification information. RFID tags can be either active, battery-assisted passive, or passive. Those that are active or battery-assisted passive require a battery to aid in power supply. However, a passive RFID tag harvests radio-frequency (RF) energy transmitted from an RFID reader to power itself and to communicate via backscatter radio communication (Dobkin, 2008). This energy harvesting involves connecting an antenna to a charge pump circuit. The antenna receives RF energy. The RF energy is then rectified into direct current (DC) power. After the conversion, the DC power can be used to operate a load. All of the components utilizing the DC power can be modeled together as one load at the charge pump's output. This load affects the matching of the charge pump affecting the amount of power the charge pump is able to convert from RF into DC. Furthermore, the charge pump is not lossless due to its intrinsic inefficiency, parasitic and resistive losses in the diodes, and radiation. Characterization of charge pump circuits assists in the optimization for a given load and input power and leads to designing more efficient charge pumps. The measurement and characterization of a 4-stage Dickson charge pump is the main focus of this paper.



DICKSON CHARGE PUMP

Passive RFID tags typically use some variant of the Dickson charge pump to increase voltage after harvesting RF energy (Trotter, 2009b). Power received by the RF tag's antenna is coupled into a charge pump. There, the RF power is rectified by means of the first stage of the charge pump, the diode-capacitor couple D1 and C1, as shown in Figure 1. The stages are denoted by perpendicular diode-capacitor pairs. The diode acts as a gate allowing current to flow in the forward direction only.

Figure 1. Schematic of a Four-Stage AC-DC Dickson Charge Pump.



The charge pump's operation can be analyzed by investigating when the input AC voltage is positive or negative. During the positive cycle of the AC voltage, diodes D2 and D4 turn on upon reaching the diode threshold voltage. This allows current to pass through the diodes and charge the capacitors. In the negative cycle, diodes D2 and D4 turn off, and diodes D1 and D3 turn on and continue to charge the capacitors. When parameters vary the following equation describes how the output voltage behaves.

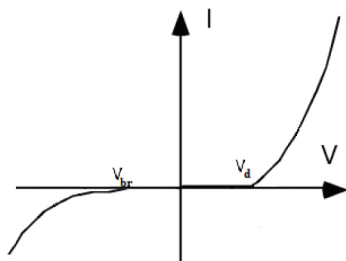
$$V_{out} = \frac{(N+1)(V_{in} - V_t)}{1 + \frac{N}{fCR_L}} \quad (1)$$

Where:

- N is the number of stages
- V_{in} is the input AC source
- V_t is the diode threshold voltage
- f is the frequency
- C is the stage's capacitance
- R_L is the resistance lost (or transferred)

Equation 1 shows a non-linear relationship between the output power and the power the charge pump receives from the receiving antenna (Trotter, 2009a). This nonlinearity is due to the presence of diodes in the circuit, which are nonlinear elements as seen in the diode I-V curve in Figure 2. To further understand the non-linear relationship between input and output power and, thus, design better, more efficient charge pumps, it is necessary to obtain data from charge pumps with varying RF frequencies, loads, and input powers.

Figure 2. Typical Current-Voltage Curve for Diodes.



IMPEDANCE MATCHING AND NON-LINEARITY

The inefficiency of the charge pump's RF to DC power conversion results in a smaller output power for the given input power. One reason for the inefficiency is reflections of power due to mismatched impedances. A matched circuit, one without difference in impedances, will result in maximum power transfer and high efficiency. In linear circuits it is possible to design a matching network that will achieve complete matching at a certain frequency due to the impedance of its elements depending solely on frequency. Another contribution to the inefficiency of the charge pump's power conversion is the impedance of a load once it is integrated with the entire circuit, changing the matching impedance.

Unlike the aforementioned linear circuits, charge pumps are nonlinear circuits due to the presence of diodes. Non-linear means complete matching only occurs at a certain input power and frequency since diode impedance depends on both factors. In practice, the input power for a charge pump will change depending on how much power the antenna is able to harvest, which varies constantly. As a consequence, the circuit's impedance is unpredictable, and it is improbable to design a specific load to match it. Therefore, measuring the efficiency with respect to varying input power and frequency allows better characterization of the expected output power for a given resistive load. This is important since loads such as RFID tags require a certain minimum input to operate.

Figure 2 shows the current-voltage relationship, of a typical diode. This non-linear relationship means that the equivalent impedance of the diode changes as a function of voltage. Two other properties of the diode that may affect the functionality of the charge pump are its threshold voltage, V_d , and reverse breakdown voltage, V_{br} . Ideally, diodes do not allow current

flow if the voltage across it is below the threshold voltage. However, if this voltage is below the reverse breakdown voltage, current flows in the opposite direction. Voltages in between V_{br} and V_d result in no current flow; therefore, they provide no power to the load.

An ideal scenario for a charge pump is one in which the receiving antenna is able to harvest enough energy to exceed the threshold voltage of the diodes and provide sufficient current to the load. The antenna's ability to harvest energy is dependent on the antenna pattern, distance from the power source, and the strength of the signal.

Since the diode is a nonlinear element, its I-V curve is consequently nonlinear as shown in Figure 2. As stated previously this non-linearity changes the equivalent impedance of the diode, which, in turn, affects the matching in the charge pump. This impedance change occurs due to the change in slope of the diode I-V curve as voltage varies. Since the impedance of the diode is proportional to the inverse of the slope, a change in the position on the curve will lead to a change in the slope and, therefore, the impedance. If the charge pump is designed to achieve complete matching at a certain frequency and at a certain input power, any deviation of one or both of these values will contribute to the mismatching of the circuit. As previously stated, the system loses power due to the mismatching between source and charge pump and inefficiencies of the charge pump itself. This relationship can be expressed by Equation (2) below.

$$\eta_{CPT} = \eta_{Matching} \eta_{CP} \quad (2)$$

Where:

η_{CPT} is the efficiency of the total charge pump system.

$\eta_{Matching}$ is the ratio of the transmitted power into the charge pump to the total power.

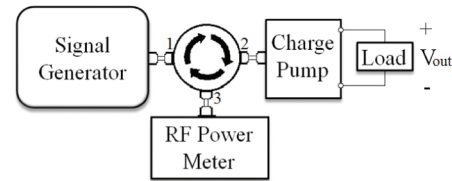
η_{CP} is the efficiency of the charge pump itself.



MATERIALS AND METHODS

In order to characterize the charge pump, the charge pump output voltage and input voltage were measured as a function of transmitted power, frequency, and load impedance. The measurement system was composed of a signal generator (Model E8247C Agilent), a circulator (Model F2658-0600-67 Wentec), an RF power meter (Model E4418B Agilent), and a charge pump as shown in Figure 3. The charge pump was a Four-Stage Dickson Charge Pump containing Avago HSMS2862 diodes and 10 pF RF capacitors on a four layer FR-4 board with 50 Ω traces at 5.8 GHz.

Figure 3. Schematic of the test system.



As the charge pump was mismatched, some of the incident power was reflected. The circulator assists with measuring this reflected power. Circulators are passive, three port devices where the energy entering any one port is transferred to another port. Thus in Figure 3, the power from the signal generator enters port one and exits port two into the charge pump. Reflected energy from the charge pump enters the circulator's port two and exits port three into the RF power meter. It was assumed that no power was reflected out of the RF power meter. Each time a signal passes through the circulator, it experiences loss since the circulator is a lossy device. Since the measured signal passes from the signal generator through the circulator to the charge pump and from the charge pump to the RF power meter, it experiences this loss term twice. Therefore, the power absorbed by the charge pump can be calculated by Equation 3:

$$P_{in} = P_{SigGen} - 2L_{circ} - P_{RfMeter} \quad (3)$$

Where:

P_{in} is the power absorbed by the charge pump.

P_{SigGen} is the power generated by the signal generator.

$P_{RfMeter}$ is the power recorder by the RF power meter

L_{circ} is the loss inside the circulator, specified in the manufacturer datasheet to be 0.5 dB.

The charge pump efficiency was calculated by dividing the output power across the resistive load in the charge pump by the input power to the charge pump as in Equation 4 (Trotter, 2009a):

$$\eta_{CP} = \frac{P_{out}}{P_{in}} \quad (4)$$

The charge pump output power was measured across the charge pump load with a voltmeter (Model 3441A Agilent). Once the output voltage was obtained, P_{out} can be obtained from Equation 5:

$$P_{out} = \frac{|V_{out}|^2}{R_{load}} \quad (5)$$

All instruments were remotely controlled using Standard Commands for Programmable Instruments (SCPI) through the programming language for technical computing MATLAB (Matrix Laboratory). The script commanded the signal generator to be set at a specified frequency, and then it was instructed to transmit signals with power ranging from -15 dBm to 16 dBm, in increments of 1 dBm. For each value of P_{SigGen} , a measurement of V_{out} and $P_{RfMeter}$ is recorded. After the final value of 16 dBm was reached, the signal generator was set to a higher frequency and then it repeated the power emission. The frequency of operation spanned from 4.1 GHz to 7.5 GHz with a step size of 100 MHz. The charge pump under test was designed to work in the 5.8GHz Industrial Scientific and Medical (ISM) radio band. However, due to matching errors inherent to the charge pump, a wide range of frequency values were measured to observe performance both within and outside this band.



RESULTS

All efficiency results are shown in a dB scale. In this dB scale, -100 dB corresponds to a 10^{-10} % efficiency, -20 dB to a 1 % efficiency, and 0 dB to 100 % efficiency, as shown in Equation 6:

$$\text{Percentage} = 10^{\frac{dB}{10}} \quad (6)$$

Figures 4-7 represent plots of charge pump efficiency vs. frequency for different input powers with different resistive loads.

Figure 4. Efficiency vs. Frequency graph for four different input powers to the charge pump with a 100 Ω resistive load.

Figure 4. Efficiency vs. Frequency graph for four different input powers to the charge pump with a 100 Ω resistive load.

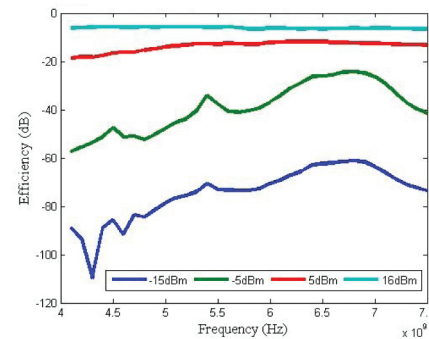


Figure 5. Efficiency vs. Frequency graph for four different input powers to the charge pump with a 1k Ω resistive load.

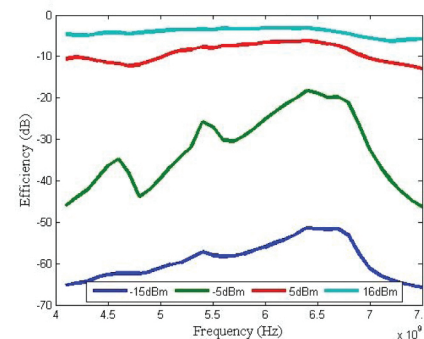


Figure 6. Efficiency vs. Frequency graph for four different input powers to the charge pump with a 20k Ω resistive load.

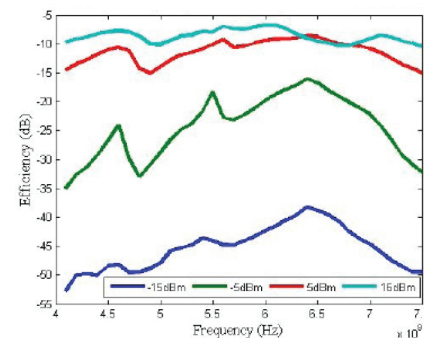
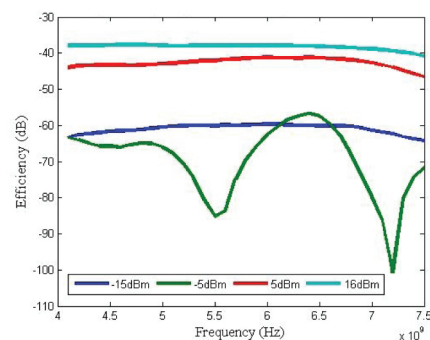


Figure 7. Efficiency vs. Frequency graph for four different input powers to the charge pump with a 500k Ω resistive load.



Figures 8-10 represent plots of charge pump efficiency vs. input power to charge pump for different resistive loads at different frequencies.

Figure 8. Efficiency vs. Power in Charge pump for various loads at 4.1 GHz

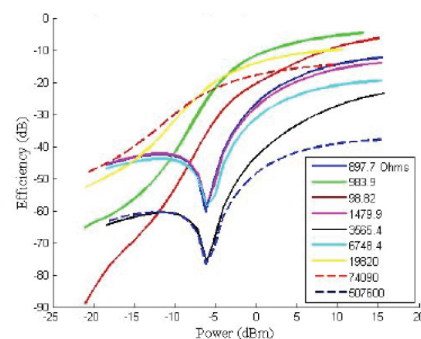


Figure 9. Efficiency vs. Power in Charge pump for various loads at 5.2 GHz

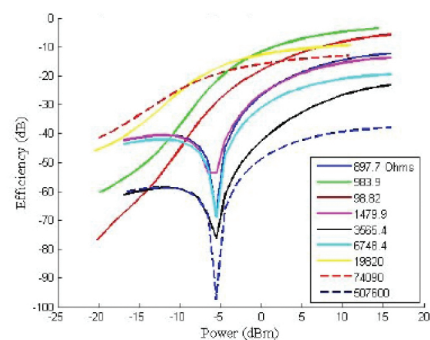
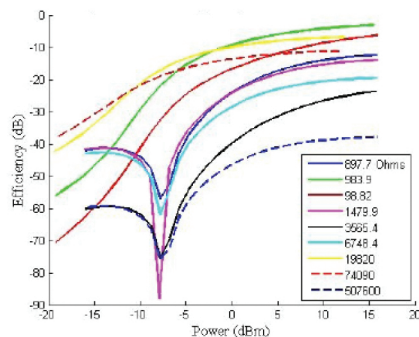


Figure 10. Efficiency vs. Power in Charge pump for various loads at 6.0 GHz



Figures 4-7 illustrate the optimal frequency of operation for different input powers. Frequencies between 6.0 GHz and 6.7 GHz produced the highest efficiencies for most resistive loads with the exception of the 20k Ω which yielded relatively higher efficiencies around 5.9 GHz. The maximum efficiency for each resistive load arises at these frequencies despite the charge pump being designed to operate at 5.8 GHz. In addition, as the input power increases resulting inefficiencies steadily increase with less erratic behavior.

Figures 8-10 show that the 1k Ω resistor yields maximum efficiency at higher powers for multiple frequencies. The absolute highest efficiency of 55.18 % was obtained at 6.0 GHz with a 1k Ω resistive load. The efficiency of the 1k Ω resistive load, however, does not remain superior as input power is decreased

For input powers less than -5 dB, 75k Ω resistive load yields maximum efficiency. Unexpected behavior is observed between -5 and -10 dBm where, for some resistance values, the efficiency of the charge pump approaches zero for all tested frequencies.



DISCUSSION

The efficiencies of the charge pump systems partly depend on matching. Since the systems studied were nonlinear, matching depends on input power, frequency, and resistive load. Therefore, the differences in efficiencies between curves are due to varying the power, the frequency, or the load.

The charge pump circuit design, which has 50 Ω micro-strip

traces at 5.8 GHz, was not best matched at 5.8 GHz. The observation that frequencies of 6.0 GHz and 6.7 GHz appear better matched than 5.8 GHz alludes to the influence of parasitic elements which affect the matching frequency of the circuit. Since parasitic elements change the equivalent impedance of the charge pump circuit elements, accounting for these parasitics more accurately will aid in creating a charge pump circuit that is best matched at 5.8 GHz. In addition, understanding the effects of parasitics will aid in better design methods for specific input powers.

As the input power increases over 5 dBm, the efficiencies saturate. It is hypothesized that the reason for this small increase in efficiency is due to a decrease in the slope's rate of change of the diode's I-V curve as voltage increases. Figure 2 shows that at higher voltages, the I-V curve approaches linearity. In other words, the slope changes less as voltage increases which implies that the equivalent impedance of the diode changes less. Therefore, a decreased change in efficiency is expected. At these higher input powers, the diode can be modeled as a linear element which implies that the impedance can be approximated as constant. Therefore, if the circuit becomes linear as input power increases, then only frequency should affect the matching of the circuit and not power. This independence of input power on matching at higher input powers implies that the matching efficiency of the circuit will not vary as input power increases and therefore the charge pump efficiency should reach a saturation limit.

The unexpected drop in efficiency that occurs between -5 dBm and -10 dBm in Figures 8-10 may be explained by the equivalent impedance of the diodes at these input powers. At low input powers, the slope of the diode's I-V curve changes more rapidly than at high powers; resulting in a change in impedance. If this change in impedance diverges away from the matching impedance of the diode, then the efficiency of the charge pump significantly decreases. Another possibility is that parasitic capacitances and/or inductances of the diode are causing the dip. The equivalent impedance of the diode may be changing from capacitive to inductive as the input power decreases. This change from capacitive to inductive implies that at one particular input power, the equivalent impedance of the diode is purely resistive. At this resonant power, the capacitive and inductive parasitics of the diode cancel each other. This purely resistive equivalent impedance of the diode implies that maximum power loss occurs since all the energy-storage characteristics of the diode are absent at the resonant power. Non-reson-

ant input powers result in a diode whose equivalent impedance is not purely resistive. Therefore, it is expected that the dip only occurs when this resonant power is reached.

From characterizing the 5.8 GHz four-stage Dickson charge pumps, it can be determined what input values are necessary for obtaining certain efficiencies or certain output powers. Certain RFID tags, such as the UHF Symbol® Class 0, Gen 1 that operates at 915 MHz, require a minimum of -10 dBm to turn on (Banerjee, 2007). Therefore, since the RFID tag's electronics represent a certain equivalent resistance, the charge pump must be designed to operate with this load impedance at the allotted frequency such that at least -10 dBm is produced to power this RFID tag.



FUTURE WORK

The current work has demonstrated a flexible system to characterize charge pumps. To understand how to design a more efficient charge pump, future work will involve the study of charge pumps with various stages, capacitances, diodes, and matching networks. To make these tests more modular, a board with multiple charge pumps will be constructed. Although there are many factors that contribute to the outcome, developing a mathematical model based on simulations to justify these results would aid in designing more of efficient charge pumps.

Input powers higher than 16 dBm can be tested in order to verify the hypothesis that the charge pump efficiency reaches a saturation limit as input power increases. If the saturation occurs, it is most likely due to the diode entering the linear region of its I-V curve but further researching is needed to verify this.

To test the unexpected decrease in efficiency as shown in Figures 8-10, an appropriate model of the diodes in the four-stage Dickson charge pump that incorporates parasitic effects should be used. If this model is accurate enough, the resonant power at which the equivalent impedance of the diode becomes purely resistive can be determined. If this hypothesis is correct, a significant decrease in efficiency at this resonant power is expected.



REFERENCES

- Akyildiz, I.F., Su, W., Sankarasubramaniam, Y., Cayirci, E. (2002). Wireless Sensor Networks: a Survey. *Computer Network.*, 38, 393-422.
- Banerjee, S. R., Jesme, R., & Sainati, R. A. (2007). Performance Analysis of Short Range UHF Propagation as Applicable to Passive RFID. *IEEE International Conference on RFID*, 33.
- Dobkin, D. (2008). *The RF in RFID: Passive UHF RFID in Practice*. Elsevier.
- Finkenzeller, K. (2003). *RFID Handbook: Fundamentals and Applications in Contactless Smart Cards and Identification*. 2nd ed., 1.
- Lee, D., Kim, S., & Kim, H. (2010). Mobile Platform for Networked RFID Applications. *Information Technology: New Generations (ITNG)*, 2010 Seventh International Conference on , 625-630.
- Trotter, M. S. (2009a). Effect of DC to DC Converters on Organic Solar Cell Arrays for Powering DC Loads. 12-15.
- Trotter, M. S., Griffin, J.D., Durgin G. D. (2009b). Power-Optimized Waveforms for Improving the Range and Reliability of RFID Systems. 1-2.
- Wentec Microwave Corp. Coaxial RF circulator: F2658. Retrieved from <http://www.wenteq.com/Ferrite-pdfs/F2658.pdf>